XI International Conference on Computational Plasticity. Fundamentals and Applications
COMPLAS XI
E. Oñate, D.R.J. Owen, D. Peric and B. Suárez (Eds)

NUMERICAL SIMULATION OF DYNAMIC PORE FLUID-SOLID INTERACTION IN FULLY SATURATED NON-LINEAR POROUS MEDIA

H. SABETAMAL[†*], M.NAZEM [†], S.W. SLOAN[†] AND J.P.CARTER[†]

[†] Centre for Geotechnical and Materials Modelling
The University of Newcastle
Callaghan 2308, NSW, Australia
www.newcastle.edu.au/research-centre/cgmm/
[*]e-mail: Hassan.Sabetamal@uon.edu.au

Key words: Large strain, ALE method, Saturated soils, Dynamic consolidation.

Abstract. In this paper, a large deformation formulation for dynamic analysis of the pore fluid-solid interaction in a fully saturated non-linear medium is presented in the framework of the Arbitrary Lagrangian-Eulerian method. This formulation is based on Biot's theory of consolidation extended to include the momentum equations of the solid and fluid phases, large deformations and non-linear material behaviour. By including the displacements of the solid skeleton, **u**, and the pore fluid pressure, **p**, a (**u**-**p**) formulation is obtained, which is then discretised using finite elements. Time integration of the resulting highly nonlinear equations is accomplished by the generalized–α method, which assures second order accuracy as well as unconditional stability of the solution. Details of the formulation and its practical implementation in a finite element code are discussed. The formulation and its implementation are validated by solving some classical examples in geomechanics.

1 INTRODUCTION

In quasi-static analysis it is common to assume that soil behaves as either a drained or an undrained medium. Under these conditions a single phase description of the porous medium may provide reasonable and acceptable results. However, in many cases the fully drained or undrained assumptions may lead to inaccurate results due to partial consolidation occurring in the soil, which generally depends on the hydraulic conductivity of the soil as well as the rate of applied loading. By using an analytical solution for dynamic consolidation problems in a **u-p** formulation, Zienkiewicz *et al* [1] investigated the conditions under which the undrained or quasi-static assumptions can be safely used. For conditions that are intermediate between fully drained and undrained, in which consolidation of the soil will take place, there is an interaction between the solid soil skeleton and the pore fluid flow. Consequently, the equations of motion for the individual constituents involve interaction terms and the stresses, both total and effective, depend on the kinematics of both phases.

Biot[2] presented one of the first theories governing the behaviour of saturated porous media. Later, Small *et al.*[3] and Prevost [4] extended Biot's theory into the material and geometrically non-linear regimes, respectively. Zienkiewicz and Shiomi [5] conducted a comprehensive study on solutions of the Biot-type formulation and summarised different analysing methods in three categories namely the (a) **u**-**p**, (b) **u**-**U** and (c) **u**-**p**-**U** formulations. Here **u**, **p**, and **U** represent the soil skeleton displacements, the pore fluid (water) pressure and the pore fluid (water) displacements, respectively. The finite element method (FEM) facilitates the discretisation of the governing differential equations in the space domain and makes it possible to extend the theory to employ elastoplastic nonlinear constitutive models in order to obtain reliable solutions for displacements and pore water pressures. This study presents an application of the FEM to solve dynamic coupled consolidation problems involving material nonlinearity as well as large deformations. Such an analysis requires a robust time marching scheme. The generalized-α algorithm (CH) developed by Chung and Hulbert [6] is an implicit integration scheme that possesses the necessary conditions of a standard time integration algorithm such as unconditional stability, second order accuracy and numerical damping capability. Kontoe *et al.*[7] used this scheme to solve coupled problems of geomechanics. The ability of this method in solving dynamic consolidation problems in geomechanics, particularly in an Arbitrary Lagrangian-Eulerian framework, is investigated in this paper.

Among others, two main sources of nonlinearity, namely material nonlinearity and geometric nonlinearity, can arise in the analysis of porous continua. Geometric nonlinearity is important in many cases such as the analysis of liquefaction, deep penetration of objects into soil layers, and any situation where the strain level is relatively high. This kind of analysis usually involves severe mesh distortion and, therefore, the Lagrangian finite element methods normally fail to provide a complete solution, usually due to the eventual development of a negative Jacobian in some elements. On the other hand, the Arbitrary Lagrangian-Eulerian (ALE) method has been developed to eliminate mesh distortion. In this study the ALE method presented by Nazem *et al.*[8, 9] is employed to solve dynamic consolidation problems of geomechanics in which the pore fluid interacts with the solid soil skeleton. The first part of this paper briefly describes the governing equations of the saturated porous medium. Time discretization of the governing equations is then presented using the CH method, followed by implementation of the approach in a finite element code. Finally, some numerical examples are presented in order to validate the implementation of the theoretical framework and to demonstrate its application in practice.

2 FINITE ELEMENT FORMULATION

The global equations governing the dynamic consolidation of a porous medium can be obtained by combining the overall momentum balance equation of the solid-fluid phase, the momentum balance equation for the pore fluid and the continuity of mass through the principle of effective stresses and the Darcy's law resulting in the following set of equations (e.g., Zienkiewicz *et al.*[5])

$$\mathbf{M}\ddot{\mathbf{u}} + \mathbf{C}\dot{\mathbf{u}} + \mathbf{K}_{ep}\mathbf{u} + \mathbf{L}\mathbf{p} = \mathbf{f}^{u} \tag{1}$$

$$\mathbf{L}^{T}\dot{\mathbf{u}} + \mathbf{S}\dot{\mathbf{p}} - \mathbf{H}\mathbf{p} = \mathbf{f}^{p} \tag{2}$$

where **M**, **C** and $\mathbf{K}_{ep}$ are, respectively, the mass matrix, the damping matrix, and the elastoplastic stiffness matrix of the solid soil skeleton. **L**, **H**, and **S** represent, respectively, the coupling matrix, the flow matrix, and the compressibility matrix. $\mathbf{f}^{u}$ is the vector of external nodal forces and $\mathbf{f}^{p}$ is a fluid supply vector. Classical finite-element algorithms used in geomechanics usually assume that only small strains occur in the soil. However, this assumption is no longer valid for large deformation problems. Finite element approaches often use an Updated-Lagrangian (UL) formulation to incorporate the effects of finite deformations as well as the volume changes in a large-deformation analysis. However, the UL method fails to provide a solution in problems with relatively large displacements due to mesh distortion. Nonetheless, this method is the main engine of the ALE operator split technique presented in Section 4 of this paper, and thus a brief description of the time-stepping scheme employed to solve the governing equations in an UL framework is given in next section.

3 TIME INTEGRATION

Finite element discretisation of the global equations leads to a system of second-order ordinary differential equations in which time is a continuous variable. In a direct time-integration scheme, Equation (1) is integrated by a numerical step-by-step procedure. Newmark's scheme is one of the most popular methods in the family of direct time integration techniques. In this method, the displacements and velocities at time t_{n+1} can be approximated by

$$\mathbf{u}_{n+1} = \mathbf{u}_n + \Delta t\dot{\mathbf{u}}_n + \frac{\Delta t^2}{2}[(1-2\beta)\ddot{\mathbf{u}}_n + 2\beta\ddot{\mathbf{u}}_{n+1}] \tag{3}$$

$$\dot{\mathbf{u}}_{n+1} = \dot{\mathbf{u}}_n + \Delta t[(1-\gamma)\ddot{\mathbf{u}}_n + \gamma\ddot{\mathbf{u}}_{n+1}] \tag{4}$$

where β and γ are integration parameters. However, Newmark's method cannot predict high-frequency modes accurately. Thus, numerical damping is introduced to eliminate spurious high frequency oscillations whilst preserving the important low frequency modes. Algorithmic damping can be introduced to Newmark's scheme by increasing the value of γ (larger than 0.5) and selecting the smallest value of β compatible with the stability requirements[10]. However, algorithmic damping influences the low-frequency behaviour, corresponding to a reduction of the accuracy to first order. By using averages with different degrees of forward weighting on the different terms in the equation of motion, the low-frequency properties can be improved, while retaining high-frequency damping. Three different schemes have been investigated in detail: forward weighing of the stiffness and load terms by Hilbert *et al.*[11], forward weighting of the inertial term by Wood *et al.*[12] and different forward weighting of the stiffness and the inertial terms by Chung and Hulbert [6]. In the last of these methods, which is known as the generalized-α or CH method, the inertia terms are evaluated at time $t = t_{n+1-\alpha_m}$ of the considered interval Δt, whereas all other terms are evaluated at some earlier time $t = t_{n+1-\alpha_f}$ ($\alpha_f \geq \alpha_m$). Therefore, using this method equation (1) can be written as

$$\mathbf{M}\ddot{\mathbf{u}}_{n+1-\alpha_m} + \mathbf{C}\dot{\mathbf{u}}_{n+1-\alpha_f} + \mathbf{K}\mathbf{u}_{n+1-\alpha_f} + \mathbf{L}\mathbf{p}_{n+1-\alpha_f} = \mathbf{f}_{n+1-\alpha_f} \tag{5}$$

where

$$\ddot{\mathbf{u}}_{n+1-\alpha_m} = (1-\alpha_m)\ddot{\mathbf{u}}_{n+1} + \alpha_m\ddot{\mathbf{u}}_n \tag{6}$$

$$\dot{\mathbf{u}}_{n+1-\alpha_f} = (1-\alpha_f)\dot{\mathbf{u}}_{\mathrm{n}+1} + \alpha_f\dot{\mathbf{u}}_{\mathrm{n}} \tag{7}$$

$$\mathbf{u}_{n+1-\alpha_f} = (1-\alpha_f)\mathbf{u}_{\mathrm{n}+1} + \alpha_f\,\mathbf{u}_{\mathrm{n}} \tag{8}$$

$$\mathbf{p}_{n+1-\alpha_f} = (1-\alpha_f)\mathbf{p}_{n+1} + \alpha_f\,\mathbf{p}_n \tag{9}$$

$$\mathbf{f}_{n+1-\alpha_f} = (1-\alpha_f)\mathbf{f}_{n+1} + \alpha_f\,\mathbf{f}_n \tag{10}$$

The governing equations of the **u-p** formulation, defined here as equations (1) and (2), can now be discretised. Equation (1) can be written in incremental form at time $t = t_{n+1}$ as

$$\mathbf{M}\Delta\ddot{\mathbf{u}} + \mathbf{C}\Delta\dot{\mathbf{u}} + \mathbf{K}_{ep}\Delta\mathbf{u} + \mathbf{L}\Delta\mathbf{p} = \mathbf{f}^{u} - {}^{t}\mathbf{f}_{int} - \mathbf{M}\ddot{\mathbf{u}}_n - \mathbf{C}\dot{\mathbf{u}}_n \tag{11}$$

and according to the CH method

$$\mathbf{M}\Delta\ddot{\mathbf{u}}_{n+1-\alpha_m} + \mathbf{C}\Delta\dot{\mathbf{u}}_{n+1-\alpha_f} + \mathbf{K}\Delta\mathbf{u}_{n+1-\alpha_f} + \mathbf{L}\Delta\mathbf{p}_{n+1-\alpha_f} = \mathbf{f}^{u}_{n+1-\alpha_f} - {}^{t}\mathbf{f}_{int} - \mathbf{M}\ddot{\mathbf{u}}_n - \mathbf{C}\dot{\mathbf{u}}_n \tag{12}$$

where ${}^{t}\mathrm{f}_{\mathrm{int}}$ denotes the internal forces at the previous time step ($t=t_n$).
Expressing Equations (6~9) in incremental form and substituting them in Equation (12) yields:

$$\frac{(1-\alpha_m)}{(1-\alpha_f)}\mathbf{M}\Delta\ddot{\mathbf{u}} + \mathbf{C}\Delta\dot{\mathbf{u}} + \mathbf{K}\Delta\mathbf{u} + \mathbf{L}\Delta\mathbf{p} = \frac{1}{(1-\alpha_f)}\left[\mathbf{f}^{u}_{n+1-\alpha_f} - {}^{t}\mathbf{f}_{int} - \mathbf{M}\ddot{\mathbf{u}}_n - \mathbf{C}\dot{\mathbf{u}}_n\right] \tag{13}$$

Similarly, Equation (2) may be written as

$$\mathbf{L}^{T}\dot{\mathbf{u}}_{n+1} + \mathbf{S}\dot{\mathbf{p}}_{n+1} - \mathbf{H}\mathbf{p}_{n+1} = \frac{1}{(1-\alpha_f)}\left[\mathbf{f}^{p}_{n+1-\alpha_f} - \alpha_f\mathbf{L}^{T}\dot{\mathbf{u}}_n - \alpha_f\mathbf{S}\dot{\mathbf{p}}_n + \alpha_f\mathbf{H}\mathbf{p}_n\right] \tag{14}$$

Newmark's recurrence relations in (3) and (4) can be written in incremental form as

$$\Delta\ddot{\mathbf{u}} = \frac{\Delta\mathbf{u} - \mathbf{u}^{l}}{\beta\Delta t^{2}} - \ddot{\mathbf{u}}_n \tag{15}$$

$$\Delta\dot{\mathbf{u}} = \dot{\mathbf{u}}^{l} - \frac{\gamma}{\beta\Delta t}(\mathbf{u}^{l} - \Delta\mathbf{u}) - \dot{\mathbf{u}}_n \tag{16}$$

Moreover, the pore water pressure at $t = t_{n+1}$ can be estimated by a first order approximation as[13]

$$\Delta\mathbf{p} = \mathbf{p}^{l} + \theta\Delta t\dot{\mathbf{p}}_{n+1} \tag{17}$$

Note that $\mathbf{u}^{l}$, $\dot{\mathbf{u}}^{l}$ and $\mathbf{p}^{l}$ appearing in the above Equations are considered as auxiliary variables to simplify the formulation, and they contain the known variables from the previous time step as

$$\mathbf{u}^{l} = \Delta t\dot{\mathbf{u}}_n + \frac{\Delta t^{2}}{2}(1-2\beta)\ddot{\mathbf{u}}_n \tag{18}$$

$$\dot{\mathbf{u}}^{l} = \dot{\mathbf{u}}_n + \Delta t(1-\gamma)\ddot{\mathbf{u}}_n \tag{19}$$

$$\mathbf{p}^{l} = \Delta t(1-\theta)\dot{\mathbf{p}}_n \tag{20}$$

Finally, introducing Equations (15) and (16) into Equations (13) and (14), the system of equations governing the dynamic consolidation of the continuum is obtained:

$$\begin{bmatrix} \frac{(1-\alpha_m)}{\beta\Delta t^{2}(1-\alpha_f)}\mathbf{M} + \frac{\gamma}{\beta\Delta t}\mathbf{C} + \mathbf{K}_{ep} & \mathbf{L} \\ \mathbf{L}^{\mathrm{T}} & \frac{\beta\Delta t}{\gamma}(\frac{\mathbf{S}}{\theta\Delta t} - \mathbf{H}) \end{bmatrix} \begin{bmatrix} \Delta\mathbf{u} \\ \Delta\mathbf{p} \end{bmatrix} = \begin{bmatrix} \mathbf{F}^{u} \\ \mathbf{F}^{p} \end{bmatrix} \tag{21}$$

where

$$\mathbf{F}^{u} = \frac{1}{(1-\alpha_f)}\left\{\mathbf{f}^{u}{}_{n+1-\alpha_f} + \mathbf{M}\left[\frac{(1-\alpha_m)}{\beta\Delta t^2}\mathbf{u}^{l} - \alpha_m\ddot{\mathbf{u}}_n\right] + \mathbf{C}\left[\left(1-\alpha_f\right)\left(\frac{\gamma}{\beta\Delta t}\mathbf{u}^{l} - \dot{\mathbf{u}}^{l}\right) - \alpha_f\dot{\mathbf{u}}_n\right] - {}^{t}\mathbf{f}_{int}\right\} \tag{22}$$

$$\mathbf{F}^{p} = \frac{\beta\Delta t}{\gamma(1-\alpha_f)}\left\{\mathbf{f}^{p}{}_{n+1-\alpha_f} + \mathbf{L}^{\mathrm{T}}\left[\left(1-\alpha_f\right)\left(\frac{\gamma}{\beta\Delta t}\mathbf{u}^{l} - \dot{\mathbf{u}}^{l}\right) - \alpha_f\dot{\mathbf{u}}_n\right] + \mathbf{S}\left[\frac{(1-\alpha_f)}{\theta\Delta t}\mathbf{p}^{l} - \alpha_f\dot{\mathbf{p}}_n\right] + \mathbf{H}\mathbf{p}_n\right\} \tag{23}$$

The unconditional stability of the scheme is guaranteed when

$$\alpha_m \le \alpha_f \le 0.5\ ,\ \beta \ge \frac{1+2(\alpha_f-\alpha_m)}{4}\ ,\theta > 0.5 \tag{24}$$

and second order accuracy is attained when

$$\gamma = 0.5 - \alpha_m + \alpha_f \tag{25}$$

4 ARBITRARY LAGRANGIAN-EULERIAN METHOD

In an Updated Lagrangian description of the motion of a body the mesh follows the material points. Consequently, the mesh can become excessively distorted in problems with relatively large deformations. In contrast, in an Eulerian description the mesh is fixed in space and the grid nodes are no longer coincident with material particles during the analysis. This may avoid mesh distortion but makes it difficult to describe the material boundaries. The ALE method attempts to combine the advantages of the Lagrangian and the Eulerian meshes. In this method, the computational grid does not necessarily adhere to the material points, and it can move arbitrarily. A common form of the ALE method is the operator split technique during which the analysis is performed in two steps: an Updated-Lagrangian step followed by an Eulerian step. In the first (Lagrangian) step the governing equations are solved to fulfil equilibrium and to obtain the material displacements. In the second (Eulerian) step the mesh is refined to eliminate the possible distortion. After refining the mesh, all kinematic and static variables must be transferred between the two meshes. In a coupled displacement-pore water pressure ALE analysis, the state parameters to be transformed at integration points include the effective stresses, hardening parameters, voids ratios and coefficients of permeability, while the pore-water pressures are transformed from old nodes to new nodes. The ALE operator split technique and the mesh refinement strategy used in this study were first presented by Nazem *et al.*[8] for the analysis of geotechnical problems. Nazem *et al.* [9] and Nazem *et al.*[14] applied the method to solve static consolidation problems and dynamic problems involving large deformations, respectively.

5 NUMERICAL EXAMPLES

The numerical time-integration scheme explained in Section 3 has been implemented into SNAC, a finite element code developed by the geomechanics group at the University of Newcastle, Australia. SNAC was used to analyse the two numerical examples presented in this section.

5.1 One-dimensional finite elastic consolidation

In order to validate the coupled formulation presented here, we study a 10 m deep column of fully saturated soil and we compare the results with available analytical and numerical solutions. Figure 1 shows the geometry of the problem as well as the boundary conditions and applied load types. To simulate one-dimensional behaviour all nodes are restrained in the horizontal direction. Drainage can only take place through the top boundary of the model.

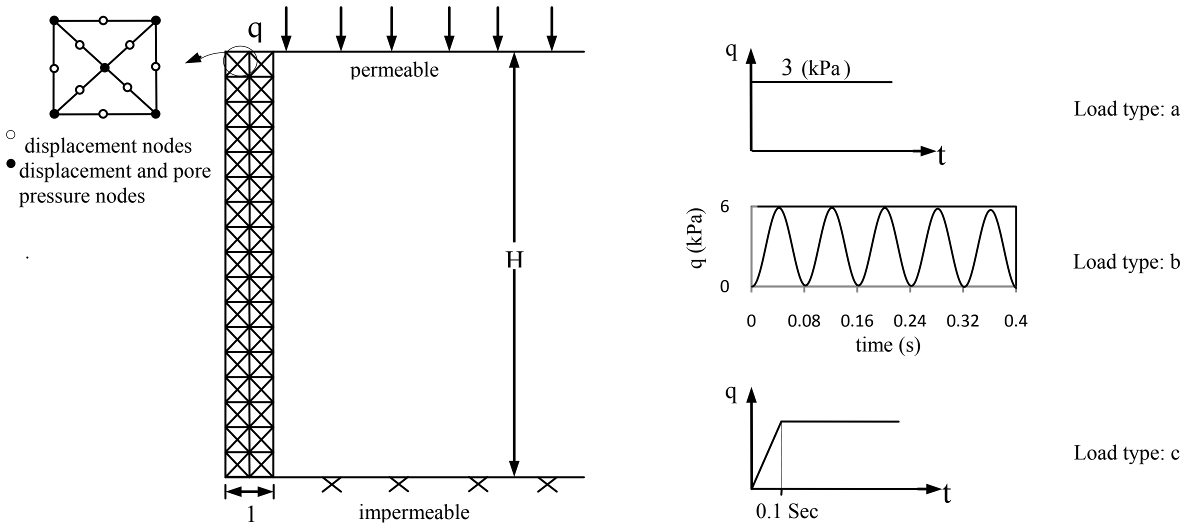

Figure 1: One-dimensional dynamic consolidation problem

de Boer[15] presented an analytical solution for a one dimensional transient wave propagation problem under a time-dependent load assuming small strains, an elastic material model and an incompressible pore fluid. The response of the soil column to step loading (type a) as well as a sinusoidal loading (type b) is investigated here. The material parameters are in accordance with de Boer[15], i.e., the Young's modulus of the soil is $E = 30$MPa, Poisson's ratio $\upsilon = 0.2$, the soil porosity $n = 0.33$ and the permeability $k = 0.01$m/s. Figure 2a shows the vertical displacement of the soil column versus time due to load type (a) and at depths 0.0 and 1.0m, whereas Figure 2b depicts the response of the pore water pressure at different depths and times. Figure 2 shows that the results obtained in this study are in good agreement with the analytical solution. For the case of a sinusoidal load, the pore water pressure response is plotted versus time in Figure 3, which indicates negative values (suction) in the vicinity of the loading surface. According to de Boer[15] this result is due to the recovery of the elastic skeleton matrix close to the surface during the sinusoidal loading, where the pore water does not squeeze out but is absorbed into the pores accompanied by fluid suction.

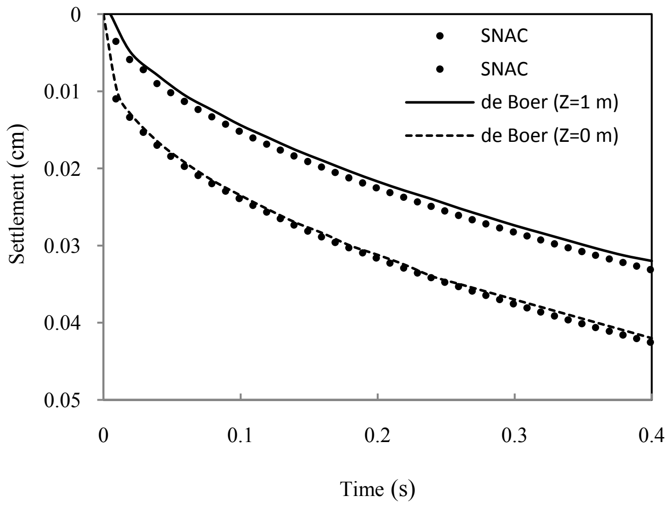

(a)

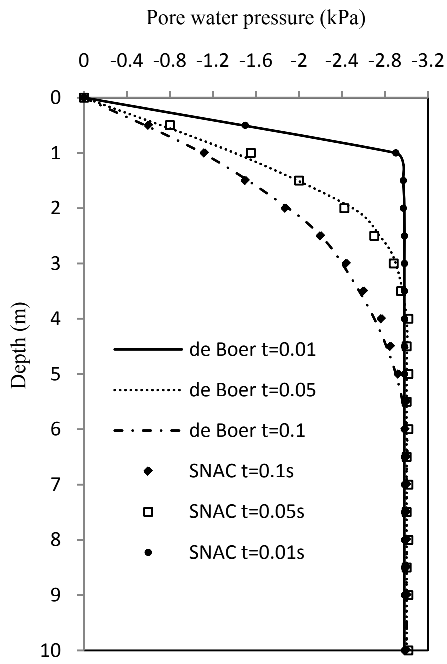

(b)

Figure 2: (a) Vertical settlement under step loading vs. time. (b) pore pressure profile of the soil column at different times.

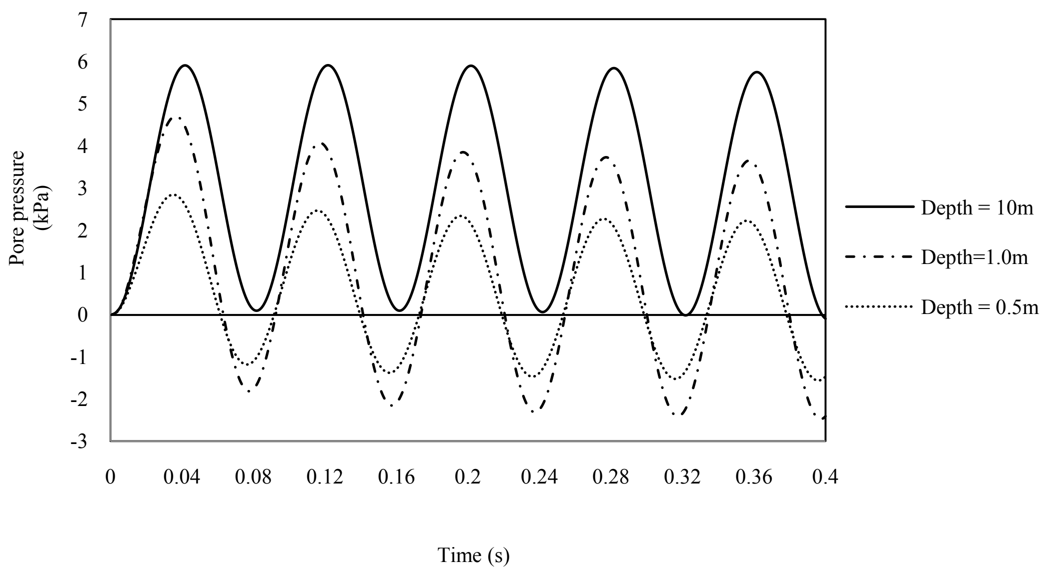

Figure 3: Response of pore water pressure vs. time to sinusoidal loading

To assess the large deformation capability of the code, the soil column was subjected to a uniformly distributed step load q at the free surface according to the load type (c) illustrated in Figure 1. Five load levels of 0.2E, 0.4E, 0.6E, 0.8E, and 1.0E were applied on the column, and the predicted results are compared with those reported by Meroi *et al*[16]. We assume E = 1GPa, υ = 0.0, n = 0.3 and k = 0.01m/s. The applied pressure normalised by E is plotted versus the total consolidation settlements (at large time) normalized by the column depth (H) in Figure 4. The results obtained by SNAC are compared to those reported by Meroi *et al.*[16]

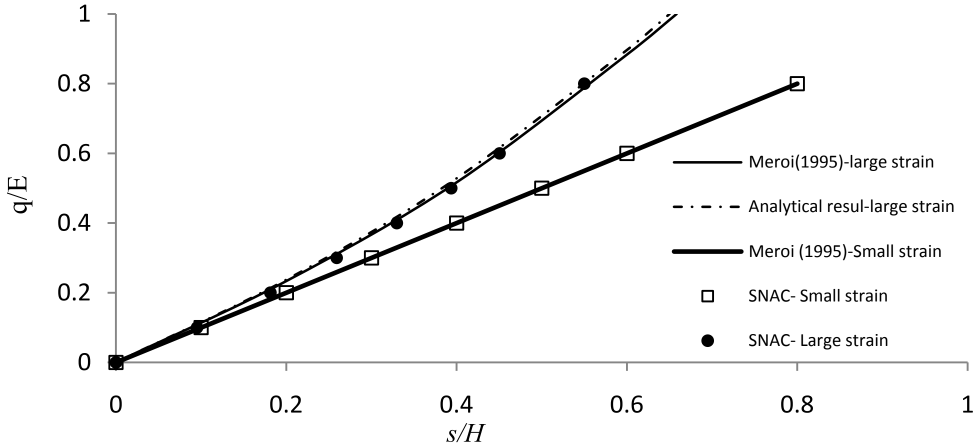

Figure 4: Normalised vertical settlement s versus load level.

5.2 Undrained analysis of a strip footing

In the second example an undrained soil layer under a rough rigid footing is considered. The mesh for the right half of the problem and the boundary conditions are shown in Figure 5. The mesh consists of 872 6-node plane strain triangular elements and 1817 nodal points. In this example we investigate the ability of the dynamic consolidation formulation to predict the undrained deformation response of the soil undergoing a dynamic load and large deformations. First we assume that the soil behaves as a Tresca material model under undrained conditions and we only consider the displacement degrees-of-freedom in the analysis. A non-associated Mohr-Coulomb material model is then used to predict the soil response by conducting a coupled consolidation analysis. Assuming zero initial geostatic stresses, the drained and undrained material properties of the soil must satisfy the following equations [17]

$$E_u = \frac{3E'}{2(1+\vartheta')} \tag{26}$$

$$\frac{c_u}{c'} = \frac{2\sqrt{N_\emptyset}}{1+N_\emptyset} \tag{27}$$

where the subscript u and the superscript ' denote an undrained and a drained quantity, respectively, c represents the cohesion of the soil, ϕ is the friction angle, E is the Young's modulus of the soil, ϑ is Poisson's ratio and N_ϕ is obtained according to

$$N_{\emptyset} = \frac{1 + sin\emptyset}{1 - sin\emptyset} \qquad (28)$$

The material parameters used here are E'/c'=200, ϑ'=0.3, ϕ' =20 and hence E_u /c_u=245, φ_u=0 (the angle of dilation), with ϑ=0.49 to simulate elastic incompressibility. A unit mass density is assumed for the soil. In the undrained analysis the load is applied at a rate of $15c_u$/s, i.e., a total uniform pressure $15c_u$ is applied on the footing in 1 second. The settlement of the footing, normalised by its half width, is plotted versus the applied pressure, normalised by c_u, in Figure 6. A clear collapse load, similar to the Prandtl's undrained collapse load at small strain, q = 5.14c_u, is not identifiable in this analysis. The higher soil stiffness predicted by the dynamic analysis results from inertia effects alone since material rate effects have not been considered in this analysis.

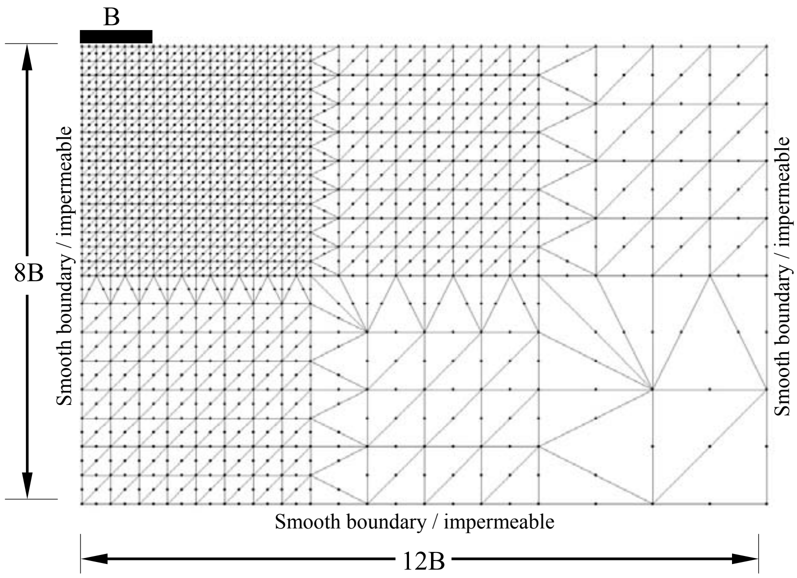

Figure 5: Rigid rough footing on a cohesive soil layer.

Similar analysis was performed utilizing the dynamic coupled consolidation algorithm with drained Mohr-Coulomb parameters, including a dilatancy angle of zero, to represent the behaviour of the soil skeleton. The soil response obtained from the dynamic consolidation analysis is also depicted in Figure 6. The results obtained from both analyses are in excellent agreement. It is worth noting that the large deformation results presented in Figure 6 were obtained by the ALE method and the UL method could not simulate the dynamic response under rapid loading due to the severe mesh distortion.

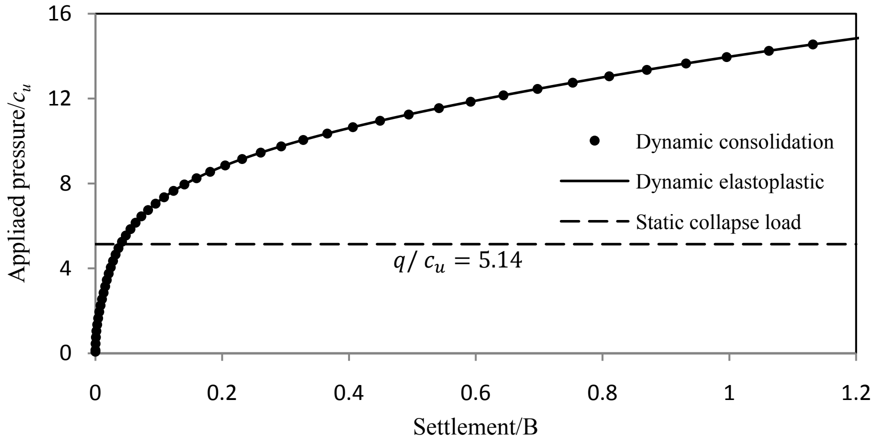

Figure 6: Load-displacement curves

6 CONCLUSIONS

A numerical procedure for the analysis of dynamic consolidation problems involving material nonlinearity as well as geometrical nonlinearity was presented in this study. Dynamic coupled equations were discretised in the time domain by using the generalized-α method, and the numerical algorithm was implemented in a finite element code. For the problems solved, the numerical results are in a good agreement with results available in the literature and analytical solutions. Also, it was shown that the generalised-α method can be used in large deformation analysis of consolidation problems with dynamic loads.

REFERENCES

[1] Zienkiewicz, O.C., Chang, T. and Bettess, P. Drained, undrained, consolidating and dynamic behaviour assumptions in soils. *Géotechnique* (1980) **30**(4):385-395.

[2] Biot M.A. General theory of three dimensional consolidation. *Journal of Applied Physics* (1941) **12**:155–164.

[3] Small, J.C., Booker, J.R and Davis, E.H. Elastoplastic consolidation of soils. *International Journal of Solids and Structures*, (1976), **12**:431-448.

[4] Prevost, J.H. Nonlinear transient phenomena in saturated porous media. *Computer Methods in Applied Mechanics and Engineering* (1982) **20**:3-18.

[5] Zienkiewicz, O.C. and Shiomi, T. Dynamic behaviour of saturated porous media; The generalized Biot formulation and its numerical solution. *International Journal for Numerical and Analytical Methods in Geomechanics.* (1984) **8**:71-96.

[6] Chung, J. and Hulbert, G.M. A time integration algorithm for structural dynamics with improved numerical dissipation: the generalized-α method. *Journal of Applied Mechanics.* (1993) **60**:371–375.

[7] Kontoe, S. Development of time integration schemes and advanced boundary conditions for dynamic geotechnical analysis. *Ph.D. Thesis, University of London.* (2006)

[8] Nazem, M. Sheng, D. and Carter, J.P. Stress integration and mesh refinement in numerical solutions to large deformations in geomechanics. *International Journal for Numerical Methods in Engineering.* (2006) **65**:1002-1027.

[9] Nazem, M. Sheng, D. Carter, J.P. and Sloan, S.W. Arbitrary-Lagrangian-Eulerian method for large-deformation consolidation problems in geomechanics. *International Journal for Analytical and Numerical Methods in Geomechanics*. (2008) **32**:1023-1050.

[10] Hughes T.J.R. Analysis of transient algorithms with particular reference to stability behavior. *In Computational Methods for Transient Analysis,* T. Belytschko and T.J.R. Hughes, Editors, North-Holland, Amsterdam,The Netherlands (1983): 67-155

[11] Hilbert, H.M. Hughes T.J.R. and Taylor R.L. Improved numerical dissipation for time integration algorithms in structural dynamics. *Earthquake Engineering and Structural Dynamics* (1977) **5**:283-292

[12] Wood, W.L. Bossak, M. Zienkiewicz, O.C. An alpha modification of Newmark's method. *International Journal for Numerical Methods in Engineering* (1981) **15**:1562-1566.

[13] Zienkiewicz, O.C. Taylor, R.L. and Zhu. J.Z. *The finite element method, its basis and fundamentals.* Elsevier, Vol. I., (2005)

[14] Nazem, M. Carter, J.P. and Airey, D. Arbitrary Lagrangian-Eulerian Method for dynamic analysis of Geotechnical Problems. *Computers and Geotechnics* (2009) **36**:549-557.

[15] de Boer, R. *Theory of porous media*. Springer, (2000)

[16] Meroi, E.A. Schrefler, B.A. Zienkiewicz, O.C. Large strain static and dynamic semi saturated soil behavior. *International Journal for Numerical and Analytical Methods in Geomechanics* (1995) **19**:81–106.

[17] Small, J.C. Elasto-plastic consolidation of soils. *Ph.D. Thesis, University of Sydney.* (1977)